Stochastic Model of Sub-Poissonian Quantum Light in an Interband Cascade Laser

Shiyuan Zhao[1,*] and Frédéric Grillot[1,2,†]

[1] *LTCI, Télécom Paris, Institut Polytechnique de Paris, 19 Place Marguerite Perey, Palaiseau 91120, France*
[2] *Center for High Technology Materials, University of New Mexico, Albuquerque, New Mexico 87106, USA*

(Received 25 May 2022; revised 23 October 2022; accepted 9 November 2022; published 9 December 2022)

This work theoretically investigates the possibility of generating amplitude-squeezed light with high-quantum-efficiency interband cascade lasers. Based on a stochastic approach, we show that, by employing the suppressed-pump-noise configuration, this kind of midinfrared source enables operation with considerable amplitude squeezing over a large bandwidth of several GHz. Our results facilitate future midinfrared quantum photonic applications such as free-space secure communications.

DOI: 10.1103/PhysRevApplied.18.064027

I. INTRODUCTION

Quantum-statistical properties of laser light have been extensively studied over the past few decades by utilizing the operator Heisenberg-Langevin equations [1], the quantum-mechanical Fokker-Planck equations [2], and the density operator master equations [3]. It was commonly acknowledged that an ideal laser operating far above the threshold generates the coherent states of light that are the eigenvectors of the annihilation operator but have dynamics most closely resembling the oscillatory behavior of a classical harmonic oscillator [4]. In a coherent state, the field fluctuations have the same amplitude in the two quadrature components (e.g., laser amplitude and phase) and minimize the product given by Heisenberg's uncertainty principle. Measurement of Poissonian photon statistics and shot-noise-limited photocurrent fluctuations characterized by an optical balanced homodyne detector [5,6] strongly support this theory. However, careful studies also revealed that lasers operating far above the threshold do not necessarily produce coherent states [7]. Other quantum states are also possible such as two-photon coherent states or squeezed states of light [8]. These pure quantum states display reduced fluctuations in one quadrature component of the coherent state at the expense of enhanced fluctuations in the other. This kind of nonclassical light is extremely useful for numerous applications that include quantum information [9], quantum-enhanced sensors [10], and ultralow noise optical communication [11].

Since the early observation of squeezed light through four-wave mixing in a pioneering experiment [12], many research groups worldwide have attempted to explore squeezed states of light with better quantum noise squeezing hence adopting diverse approaches [13]. In this context, amplitude-squeezed light from semiconductor lasers was initially proposed by Yamamoto *et al.* [14,15]. They theoretically and experimentally proved that squeezed light in lasers is achievable with a suppressed-pump-noise configuration. In this scheme, the sub-Poissonian pumping statistics of the electron current are converted directly into nonclassical photon statistics. This method can offer immense benefits in terms of wavelength, broad squeezing bandwidth, high output power, and compactness of laser diodes. While early demonstrations of amplitude-squeezed light were realized by different types of semiconductor lasers [15–17], nothing has yet been reported at midinfrared wavelengths [18]. Here, we concentrate on interband cascade lasers (ICLs) [19]. ICLs are a class of semiconductor lasers emitting in the midinfrared window (3–6 μm), which rely on the interband transition of type-II quantum wells. Moreover, such lasers are intended to take advantage of a cascading mechanism that increases the quantum efficiency and also the emitted optical power.

Hereinafter, we show that ICLs are eligible sources for the generation of amplitude-squeezed light (operating below the shot-noise level) as well as sub-Poissonian output photon statistics. Our results may further accelerate the development of an original quantum hardware in the midinfrared range, which is not yet available and that can be implemented, for instance, in the laser-based free-space secure communication systems. As is known, the atmospheric transmission spectrum holds two transparency windows, one between 3–5 μm and another between 8–14 μm. In this context, midinfrared optical sources are candidates of choice for transmission applications, especially in the case of fog or drizzle where they strongly surpass near-infrared and visible-light sources [20]. For

*shiyuan.zhao@telecom-paris.fr
†frederic.grillot@telecom-paris.fr

example, it is relevant to notice that molecular (Rayleigh) and particulate (Mie) scattering as well as the signal distortion in the atmosphere decrease at longer wavelengths [21]. Moreover, atmospheric turbulence on the propagation path seriously deteriorates the optical signal causing beam spreading, beam wandering, scintillation, or loss of spatial coherence. Numerical studies with simulated scintillation data and turbulent strength have shown the superiority of midinfrared wavelengths over near-infrared wavelengths for free-space transmissions [21]. From this perspective, there is a growing interest in the development of free-space data transfer, in particular, using quantum key distribution (QKD) protocols because current free-space communications are unidirectional and easy to eavesdrop upon. Unlike classical cryptography, continuous-variable (CV) QKD protocol is one of the major practical applications of quantum information theory that allows distribution of a key over a public channel, with security even against a computationally unlimited attacker [22]. It consists in encoding classical information into quantum signals that are exchanged between two parties connected by a quantum channel, completed by an authenticated classical channel. Very recently, this protocol already deployed in fiber optic systems has been theoretically analyzed in the context of free-space communications [23,24]. However, atmospheric turbulence causes a random variation of channel transmissivity in time hence introducing extra noise on the CV QKD systems, which decreases the secret key rate, and even renders the communication insecure in the presence of strong turbulence [25]. To overcome this problem, the operating principle of the proposed QKD channel relies on using a bright squeezed laser where the information can be exclusively encoded into a Gaussian modulation of squeezed states (e.g., in the amplitude quadrature), as schematically seen in Fig. 1. By properly doing so, one can completely eliminate information leakage to others in a reverse reconciliation scenario [26] and equally the modulation noise of the channel. Given this, using amplitude-squeezed states of midinfrared ICL is even more favorable under these circumstances because of its longer optical wavelength, large optical power as well as enhanced squeezing level and broad squeezing bandwidth. Furthermore, the modulation can be directly read out via self-homodyne detection without separate local oscillators [24], which simplifies the experimental realization. As a consequence, implementation of midinfrared squeezed ICLs can be extremely useful for the development of future satellite-based CV QKD communication links operating at longer wavelengths.

Recently, we reported a semiclassical approach based on Green's function method in order to conduct some initial investigations of ICLs' squeezing properties [27]. Our study is similar to previous descriptions [14,28] that focus on evaluating intensity squeezing with respect to the relative intensity noise (RIN) spectrum. This kind of

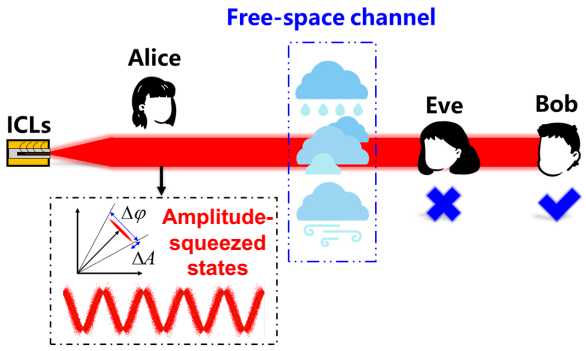

FIG. 1. Schematic representation of the midinfrared ICL system using amplitude-squeezed states for continuous-variable quantum key distribution in free-space channel.

formalism considers that the fundamental source of noise resides in the particle character of the radiation, which is treated as classical particles without mutual interaction. Shot noise is therefore not a property of the light-matter interaction, but an intrinsic property of the radiation. To this end, intensity noise fluctuations are assimilated to partition noise, which results from the coupling of the energy with the exterior of the cavity (transmission loss). Although this model has a great advantage to provide a straightforward way to describe light amplitude-squeezed states in semiconductor laser structures compared with the more complex quantum electrodynamics (QEDs), it merely introduces an alternative Langevin noise term instead of comprehensively reflecting on the granularity of photons and carriers, which means that it cannot give any information about the photon statistics and the intrinsic quantum fluctuations. To address these issues, we expand a recent stochastic model [29–31] to the case of amplitude-squeezed light generation in the midinfrared range according to the ICLs' band structure. Of note, we distinguish between intracavity photons and external output photons and emphasize the laser outcoupling process and sub-Poissonian pumping process that are crucial for the interpretation of sub-shot-noise-limited light emission. In this work, we provide a framework to permit an exact evaluation of the squeezing performance without the mathematical assumptions related to the derivation of a differential description, which predicts the laser statistical dynamics based on the Monte-Carlo algorithm. In general, it intuitively accentuates the discreteness of the changes in photons and carriers and the inherent noise of all physical processes like pumping, spontaneous emission, stimulated emission, and the transmission through the laser facet, which cannot be captured by the conventional rate equation approach [27]. Our numerical results indicate that strong intensity noise squeezing of ICLs within a bandwidth of several GHz is attainable, which certainly could be considered a promising solution for the development of midinfrared light sources with ultralow noise.

This paper is structured as follows. In Sec. II, we introduce the ICL rate equations along with the stochastic algorithm for analyzing the intensity noise squeezing. By doing so, we can discuss our results including various laser quantum characteristics and verify the accuracy with comparisons to the analytical ones in Sec. III. Prospects and conclusions are given in Sec. IV.

II. STOCHASTIC MODEL

Laser rate equations are a very well-established phenomenological approach for modeling semiconductor laser dynamics. Through the rate equations for both carrier density and photon density of the optical mode in the active region, a wealth of laser static features and dynamical characteristics can be determined with additional Langevin forces [32], including RIN properties, spectral linewidth, and the laser's response to external optical feedback effects, etc. However, the main issue when dealing with squeezed light arises from the quantum granularity of photons and carriers. The inadequacy of continuous rate equations for modeling quantum light is widely reported in the literature [33–36]. Hereinafter, we present a stochastic method based on Monte-Carlo simulations that can be employed to describe the ICLs' dynamics, including quantum squeezing properties. This method is in exact accord with the premises of the rate equation description concerning the frequency spectrum [27] yet it offers additional predictions and insights into the regime of photon distribution and other statistics features that the conventional method fails to specify.

As shown in Fig. 2, each cascading stage in ICLs contains three parts: a hole injector, an electron injector, and a *W*-configuration active region. Under the external electric field, holes and electrons flow into the active region via the tunneling effect, where they recombine through spontaneous emission, Auger recombination, and stimulated emission due to population inversion. Then, in order to replenish the carriers removed by the field, equal numbers of additional electrons and holes must be regenerated constantly and transported to the next stage. Therefore, ICLs' rate equations for carrier N and photon S can be written as

$$N_{t+1} = N_t + R_{\text{pump}} - R_{\text{st}} - R_{\text{sp}} - R_{\text{aug}}, \tag{1}$$

$$S_{t+1} = S_t + mR_{\text{st}} - R_p + m\beta R_{\text{sp}}. \tag{2}$$

Here R_{pump} is the pump rate into the active region, R_{st} and R_{sp} are the laser stimulated emission and spontaneous emission, R_{aug} is the nonradiative Auger recombination rate, $R_p = R_{\text{int}} + R_{\text{out}}$ is the laser photon decay rate, decomposed in R_{int} the photon internal decay due to internal losses and R_{out} the outcoupling rate through the laser facets, m is the cascade stage number, and β is the spontaneous emission factor.

The stochastic rate equations, Eqs. (1)–(2), capture the operating characteristics of ICLs, since each term can be related to a random event occurring inside the laser cavity, as summarized in Table I. All the values used in the simulations come from the recently developed ICL rate equation model and can be consulted in Ref. [37]. The term Γ_p is the optical confinement factor, v_g is the group velocity, g is the optical gain with a_0, N_0, and A being the differential gain, the carrier number at transparency and the area of the active region, respectively, whereas τ_{sp} is the spontaneous emission lifetime, α_{in} the internal loss, τ_{aug} the Auger lifetime, η the injection efficiency, I the pump current, q the elementary charge, and α_m the laser facet loss with L, R_1, and R_2 being the laser cavity length and power facet reflectivity.

Our simulation aims at treating photons and carriers as discrete particles N and S whose numbers fluctuate because of several events, including loss of particles (Auger recombination or photon decay), exchange of particles (emission or outcoupling process), and addition of new particles (pumping). In contrast to rate equation methods, we first establish a variety of clear-cut rules reproducing the physics of the interaction between photons and

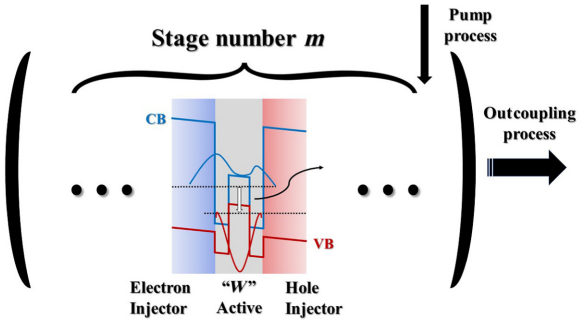

FIG. 2. Schematic representation of the ICLs' "*W*" structure of conduction band (CB) and valence band (VB) with normal (quiet) pump process.

TABLE I. Average rates of stochastic events occurring in the ICLs' rate equations [37].

Event type	Symbols	Average rate
Stimulated emission	R_{st}	$\Gamma_p v_g g S$[a]
Spontaneous emission	R_{sp}	N/τ_{sp}
Photon internal decay	R_{int}	$v_g \alpha_{\text{in}} S$[b]
Auger recombination	R_{aug}	N/τ_{aug}
Pumping	R_{pump}	$\eta I/q$
Outcoupling process	R_{out}	$v_g \alpha_m S$[c]

[a] $g = \frac{a_0(N-N_0)}{A}$.
[b] $\alpha_{\text{in}} = 5.7\ \text{cm}^{-1}$.
[c] $\alpha_m = \frac{1}{L}\log(\frac{1}{\sqrt{R_1 R_2}}) = 5.7\ \text{cm}^{-1}$.

carriers. For example, we add a certain number of carrier N into the carrier reservoir when pumping event fires and we transfer carriers to intracavity photons S_{in} during the spontaneous or stimulated emission. Afterward, we anticipate the expected number of distinct events taking place at each discrete time step in Eqs. (1)–(2). For a time increment Δt sufficiently small (e.g., we usually choose 1 ps to make sure that the noise features have been converged), the number of the ongoing events could be approximately expressed as a succession of integer random numbers drawn from the Poissonian distribution [29,38] with the Poisson parameter λ equal to the product of the corresponding average rate calculated in Table I and the time increment Δt. The construction of our model is reliable under the assumption that one occurrence of an event does not influence the probability of any other events. Generally, the basic idea of our method is to characterize photon distribution by incorporating outcoupling as an extra process along with the injection of a sub-Poissonian pumped electron. For the former, in the conventional theory, the internal field is the only "system" of interest, while the output field outside of the laser cavity is regarded as a "heat bath." Since we now are concerned about the external photon statistics, it should be treated as another "system" [14]. As a consequence, we divide photon decay into two events, outcoupling R_{out} due to the laser facet losses related to α_m and internal decay R_{in} due to all other cavity decay summarized as α_{in}. For the latter, the pumping event R_{pump} description depends on how the laser is pumped. With respect to the case of shot-noise-limited pumping or normal pumping, we take $R_{\text{pump}} = R_{\text{pump,conv}} = \eta I/q$ as a classical current source that follows a Poissonian distribution. In contrast with the case of noise-suppressed pumping or quiet pumping, the pumping term $R_{\text{pump}} = R_{\text{pump,quiet}}$ corresponds to the injection of pumped electrons with a constant rate, which is naturally related to sub-Poissonian electron statistics.

III. RESULTS

In this section, we present numerical results to illustrate our stochastic model. In the first place, we study the features of statistical dynamics in the ICLs through the second-order photon correlation function $g^{(2)}(0)$. More specifically, we show the evolution of the intracavity photon-number distributions from the chaotic (LED-like) behavior to the coherent (laserlike) one. In the second place, we demonstrate that ICLs can produce amplitude-squeezed states provided that electrical pump noise fluctuations are well suppressed. Several features such as sub-Poissonian distribution, sub-shot-noise-limited frequency spectrum, and negative Mandel Q parameter are examined to validate our theory. In addition, we verify the accuracy of our model through comparisons with an analytical approach.

A. Intracavity photon characteristics

To analyze why ICLs can naturally produce coherent states instead of amplitude-squeezed states, we start with the analysis of intracavity photon characteristics in ICLs. Above all, it is worth mentioning that photon statistics are usually described by the first two statistical moments, that is, the mean value $\langle S\rangle$ and the variance $\langle \Delta S^2\rangle = \langle S^2\rangle - \langle S\rangle^2$. There is also the second-order photon correlation function $g^{(2)}(0)$, which represents how likely two photons arrive simultaneously [4,8].

$$g^{(2)}(0) = \frac{\langle S(S-1)\rangle}{\langle S\rangle^2}. \tag{3}$$

Let us stress that for chaotic (LED) light, $g^{(2)}(0) = 2$ and for coherent (laser) light, $g^{(2)}(0) = 1$ because photon statistics follow a Poissonian distribution. Although the ICLs' photon number fluctuates at all moments during the simulation, the mean value remains unchanged, for instance, the intracavity photon number S_{in}. In Fig. 3(a), the time evolution of intracavity photon number S_{in} is shown for three different pump rates near the threshold region. We can clearly observe that the intracavity photon fluctuations are reduced when the ICLs pass from the below threshold to the above threshold. Figure 3(b) compares the stochastic simulations (diamond markers) with the analytical results obtained from the rate equation (solid lines) for mean internal photon number $\langle S_{\text{in}}\rangle$. This figure demonstrates the substantial agreement between the two approaches. It is worthwhile to highlight the sudden jumps that appear in the mean internal photon number $\langle S_{\text{in}}\rangle$ as a function of pump rate. This phenomenon is frequently referred to identify the micro- and mesolasers ($10^{-6} \leq \beta \leq 10^{-2}$) crossing the lasing threshold and especially $\beta = 10^{-4}$ for ICLs in our simulation. This feature becomes much less noticeable when it comes to the case of nanolasers for which $\beta \approx 1$ [39,40]. As depicted in Fig. 3(c), the photon correlation $g^{(2)}(0)$ also reveals the agreement between the two different methods. Only a minor deviation occurs around the ICLs' threshold. Furthermore, there is explicitly an expected transition from chaotic behavior or thermal statistics [$g^{(2)}(0) = 2$] below threshold, via intermediate statistics [$1 < g^{(2)}(0) < 2$] near threshold, to coherent behavior with Poissonian statistics [$g^{(2)}(0) = 1$] well above threshold [40]. In order to evaluate the corresponding photon distribution, we pick up the different pump rates near the threshold and make histograms of the intracavity photon number S_{in}. In Fig. 3(d), a Bose-Einstein or exponential distribution is obtained when ICLs operate below the lasing threshold. Meanwhile, in Fig. 3(f), at high pump rates, the photon distribution follows a Gaussian distribution that is a little bit wider than the Poissonian distribution with the same mean value. This deviation is generally in agreement with the earlier theoretical and experimental works [41].

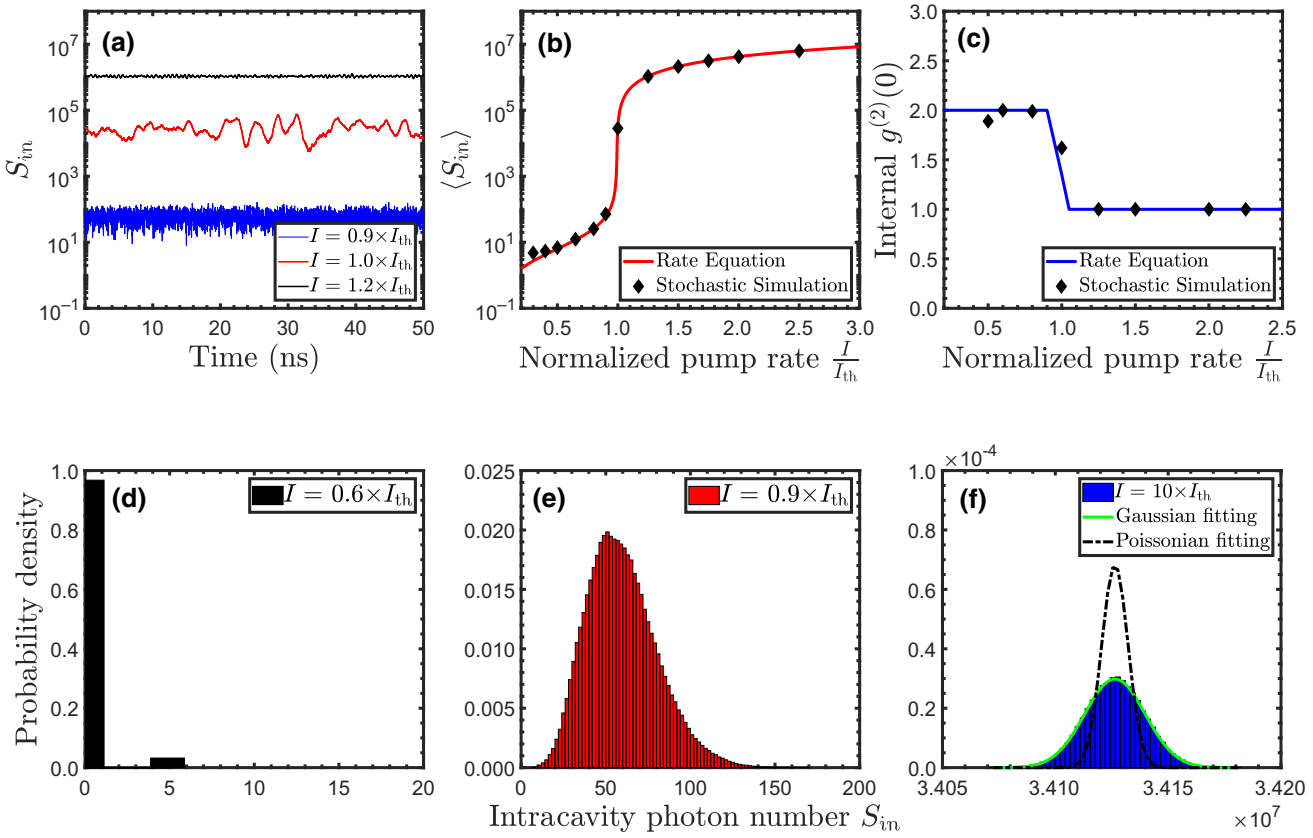

FIG. 3. (a) Time series of intracavity photon number S_{in} for three different values of pump rate near the threshold region, (b) Stochastic results (diamond markers) and analytical results from rate equations [27] (solid lines) for mean photon number $\langle S_{\text{in}}\rangle$ and also (c) internal photon correlation $g^{(2)}(0)$. Simulations for low pump rates are rejected because of statistical uncertainty. In (d) the intracavity photons show an exponential distribution. In (e) photons exhibit an intermediate distribution near the threshold. In (f) the dashed curve indicates a Poisson distribution with parameter given by the mean photon number $\langle S_{\text{in}}\rangle$ and the green curve indicates Gaussian distribution with mean and variance given by the mean photon number $\langle S_{\text{in}}\rangle$ and photon-number variance $\langle \Delta S_{\text{in}}^2\rangle$.

B. Sub-Poissonian output photon distribution

It has been widely investigated that amplitude-squeezed states can be generated from coherent states. Tremendous experimental efforts have been put into the production of those quantum states by a variety of phase-dependent nonlinear optical processes over decades, such as employing materials with large second-order ($\chi^{(2)}$) or third-order ($\chi^{(3)}$) nonlinearity through optical parametric oscillator [13] or four-wave mixing [12,42]. The recent experiment also proves the feasibility of the chip-scale squeezed-light sources by using various platforms [43–45]. Likewise, Yamamoto *et al.* proposed another way of achieving amplitude-squeezed light through the constant-current-driven semiconductor laser [15]. In this theory, when biased by a pump source with a source resistance R_S, laser differential resistance can be defined as $R_L = (dI/dV)^{-1}$ where I and V are the junction current and the junction voltage. And a photon emission event from the active region accompanies a reduction in the carrier number, which subsequently creates a junction voltage drop. This fluctuation in the voltage is recovered by a relaxation current flow in the external circuit with a time scale of $R_S C$. For the normal pump source whose resistance $R_S \ll R_L$, the junction voltage (i.e., the carrier number) recovers very quickly, so the next photon emission event is independent of the previous one, which is simply a Poisson process and therefore features the full shot noise. In contrast, for the quiet pump source whose resistance $R_S \gg R_L$, the relaxation current flows very slowly. Therefore, the next photon emission event is superimposed on the first one and consequently turns out to be the sub-Poissonian process.

The frequency histograms in Fig. 4 display the filtered output photon number S_{out} distribution with the pump current $25 \times I_{\text{th}}$ for both pump configurations. In the experiments, the photon statistics are usually measured by the photon counter, which consists, in the near-infrared range, of a sensitive detector device like an avalanche photodiode with the user-defined detection filter of duration. Here, it is worthwhile to note that we set $T_d = 100$ ps for a bit rate B of 10 Gb/s according to the relation $T_d = 1/B$ [30].

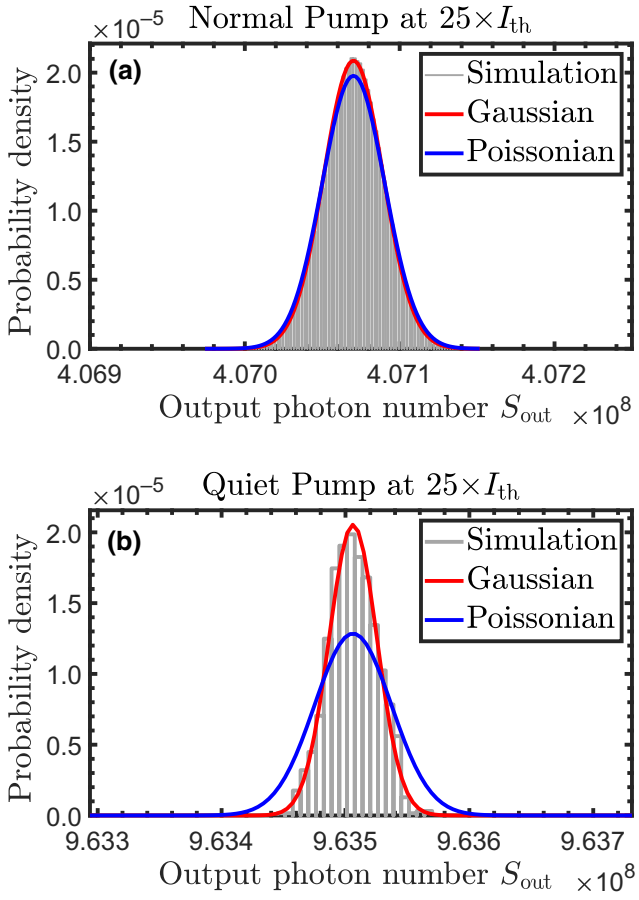

FIG. 4. Output photon number S_{out} distribution in 100-ps time slot for ICLs (a) normal or shot-noise-limited pumping and (b) quiet or noise-suppressed pumping. Red curves indicate Gaussian fitting and blue curves are Poissonian fittings with the same mean value. The pump current is set as 25 × I_{th}.

Figure 4 demonstrates the potential viability of nonclassical photon statistics in ICLs where the conventional rate equation method does not succeed. Concerning the case of normal pumping, Fig. 4(a) shows that the output photon distribution is well fitted by the Gaussian probability density function and equally by the Poissonian one with the same mean value. As for the quiet pumping, one can identify the sub-Poissonian characteristics in Fig. 4(b), which have an apparently narrower FWHM than the Poissonian one. As one can see, the maximum probability density in the Gaussian distribution is nearly twice as large as in the Poissonian one. Let us note that the slightly low output photon number for normal pumping is because of reduced electron injection rate, which is not vital for the conclusions.

C. Relative intensity noise spectra

Traditionally, the instability in the power level of semiconductor lasers is represented by RIN, which is determined as the ratio between the intensity noise power spectral density and the squared average power [32]. In an actual experiment, it can be measured by analyzing the spectrum of the photodetected signal via an electrical spectrum analyzer. Nevertheless, in order to observe the laser squeezing phenomenon, a balanced mixer detection scheme is essential since both excess noise and quantum noise of the local oscillator can be canceled out after the photoelectric signal conversion [6]. In the past decades, a series of experimental investigations have been deployed to validate this theory [15,16].

Figures 5(a) and 5(b) display the external and internal RIN spectra for normal and quiet pumping condition through Fourier transform. The parameters in Table I are still considered and the pump current is set as 2 × I_{th}. By comparing the two RIN spectra, one can find that the RIN of the outcoupled photon stays nearly the same as the intracavity counterpart at the low frequency well before the relaxation oscillation peak that has been recently observed in the previous study [46]. However, at high frequency, the external RIN approaches the so-called shot noise level (standard quantum limit) [14] whereas the internal RIN keeps decreasing as a consequence of a filtering effect, which is defined as the response function in classical laser dynamics [32]. Furthermore, considering the inset of Figs. 5(a) and 5(b), in comparison with the blue (internal RIN) and red (external RIN) curves, one may see that the noiseless pumping condition is expected to reduce the intensity noise around 10 dB. This outcome gives an implication about the generation of amplitude-squeezed states if and only if ICLs are pumped far from their threshold with a quiet current source. And the stochastic simulations perfectly agree with the previous analytical ones [27] in the regime of frequency spectra.

Figure 5(c) demonstrates the potential of sub-shot-noise-limited external RIN with the suppressed-pump-noise configuration. As aforementioned, it is desirable to use a high pump current (25 × I_{th}) without pump fluctuations to obtain amplitude-squeezed states because ICLs' differential resistance becomes much smaller in the strong forward-bias condition [47], which makes amplitude-squeezed light generation more convenient. The external RIN exhibits a strong squeezing factor of a couple of dB as well as a broad squeezing bandwidth of nearly 10 GHz. It is worth noting that ICLs should not be supposed to have an internal loss. Recently, *n*-type doping designs of ICLs can operate at ambient room temperature with internal losses α_{in} as low as 5 cm^{-1} [48], which was typically 12 cm^{-1} before the redesign. In this figure, we assume that the internal loss α_{in} approaches 1 cm^{-1} in order to get the best squeezing performance. Together, all these properties offer strong building blocks for the realization of ultralow noise laser sources at midinfrared wavelengths. For instance, as reported by a recent theoretical analysis of CV QKD protocol [24], bright amplitude-squeezed

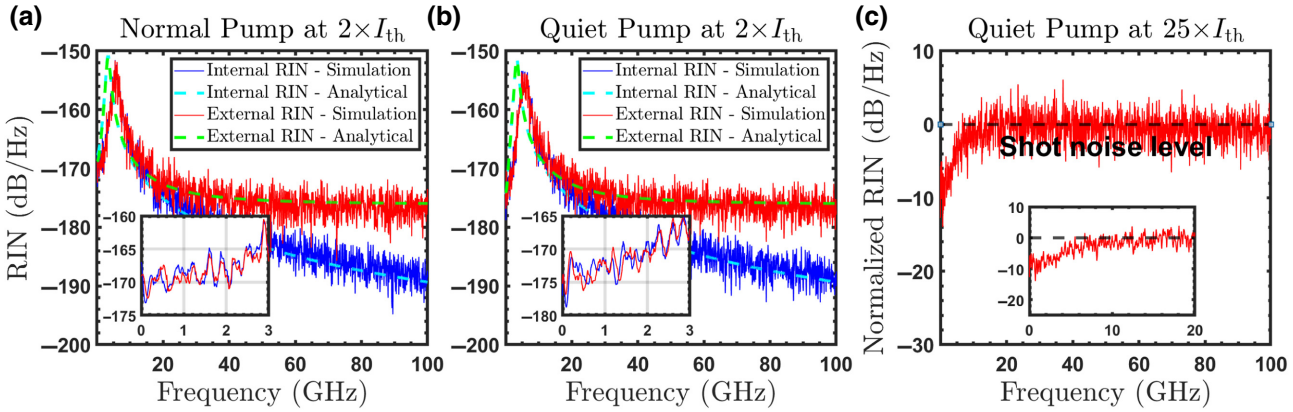

FIG. 5. Normal (a) and quiet (b) pumping condition of ICLs for both internal (blue curves) and external (red curves) RIN spectra through Fourier transform. The green and cyan dashed lines describe the previous analytical rate equation description [27]. The insets are the detailed view of those two figures within the low-frequency region. Parameters used during the simulations can be found in Table I. The pump current is fixed at $2 \times I_{th}$. (c) External RIN spectrum at $25 \times I_{th}$ but with $\alpha_{in} = 1$ cm^{-1} as an ideal condition. It should be noted that the black dashed line represents the shot noise level.

states with considerable squeezing bandwidth and level outperforms the coherent ones in different aspects, which achieve several times more significant key rates and higher robustness and tolerance up to dozens of dB for the channel loss that eventually suffices to meet the needs of downlink channels from low-earth-orbit satellites. Another point is that external RIN at the high pump rate manifests less frequency dependence than the low-pump-rate situation. This feature agrees with the prior theoretical predictions [14] and the experimental observations [49]. In a fully quantum mechanical model, the intensity noise reduction is understood as the destructive interference stemming from vacuum zero-point fluctuations and equally as the direct conversion from sub-Poissonian injected electrons to emitted photons due to laser high quantum efficiency [14].

D. The Q parameter

The Q parameter is proposed to elucidate the photon statistical properties by evaluating the divergence between the coherent Poissonian states and other possible nonclassical quantum states, which was introduced in quantum optics by Mandel [50]. This factor usually characterizes amplitude-squeezed states with negative values implying sub-Poissonian photon statistics. It is commonly defined as

$$Q = \frac{\langle \Delta S^2 \rangle - \langle S \rangle}{\langle S \rangle}. \tag{4}$$

Furthermore, another commonly used quantum factor, e.g., Fano factor, can be defined theoretically as the ratio between the variance and the mean of the output photons meanwhile experimentally as the ratio between the spectral noise power of the laser field and the shot-noise level at the same dc photocurrent of the detector. Therefore, since the Fano factor is smaller than unity, the laser field shows amplitude-squeezed quantum properties.

$$F = \frac{\langle \Delta S^2 \rangle}{\langle S \rangle} = 1 + Q. \tag{5}$$

It should be mentioned that as a result of the macroscopic ICLs' system with a large mean photon number, a very small reduction of external $g^{(2)}(0)$ below unity leads to an intensely sub-Poissonian statistics through the expression derived from second-order factorial moment:

$$g^{(2)}(0) = \frac{\langle S(S-1) \rangle}{\langle S \rangle^2} = 1 + \frac{\langle \Delta S^2 \rangle - \langle S \rangle}{\langle S \rangle^2} = 1 + \frac{Q}{\langle S \rangle}. \tag{6}$$

This effect was reported in the recent articles [51,52], which indicates that an increase in mean photon number $\langle S \rangle$ reduces the range and amplitude of antibunching [e.g., $g^{(2)}(0) < 1$]. It is because of the relationship between Q parameter and $g^{(2)}(0)$ shown in Eq. (6). However, it is still possible to maintain a good amount of photon-number noise squeezing.

Figure 6 illustrates how internal loss α_{in} plays a significant role in the amplitude-squeezing performance. Using two distinct quantum criteria namely external photon correlation $g^{(2)}(0)$ and Q parameter, our simulation highlights that the intensity squeezing factor is fundamentally limited by the internal loss of the semiconductor materials. This phenomenon can be explained by the fact that output emitted photon would be plagued by the less likely outcoupling process due to the intense competition from substantial internal loss, with the sub-Poissonian performance being thus diluted. As shown in Figs. 6(a) and 6(b), ICLs exhibit

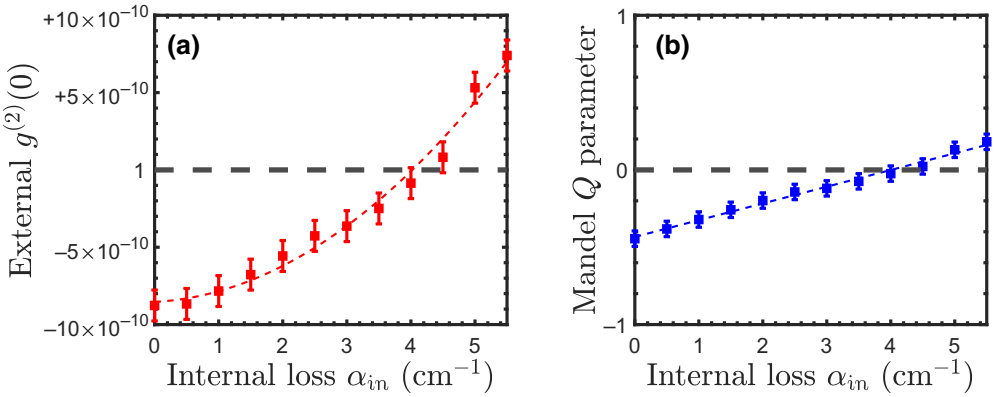

FIG. 6. (a) External $g^{(2)}(0)$ and (b) the Q parameter of the external output photons as a function of internal loss coefficient α_{in}. The measurement duration is still 100 ps and other simulation parameters remain unchanged as Fig. 5(c). In (a), an extremely slight deviation is found. Hence, for the sake of visibility, ticks of the longitudinal axis represent effectively this deviation from 1, for instance, $\pm5 \times 10^{-10}$ indicates $1 \pm 5 \times 10^{-10}$ in this case. In (b), a value of -1 manifests the maximum degree of squeezing. The black dashed line in both figures represents the shot noise level, the red (blue) dashed lines are guides for the eye, and error bars are displayed as a result of stochastic uncertainty.

clear photon antibunching characteristics or amplitude-squeezed light with negligible internal loss [$g^{(2)}(0) < 1$ and $Q < 1$]. In contrast, the squeezing properties are strongly altered with $g^{(2)}(0)$ and Q parameter both increasing, even exceeding more than 0, respectively. We can imagine that the same trend is found in the Fano factor. For this reason, it is crucial to minimize internal loss as much as possible in the future ICLs' quantum engineering design.

IV. CONCLUSIONS

In conclusion, we demonstrate that ICL is a promising candidate for generating amplitude-squeezed light in the midinfrared window with suppressed-pump-noise configuration through the analysis of sub-Poissonian photon distribution, sub-shot-noise-limited relative intensity noise spectrum, and negative Mandel Q parameter ($Q < 0$). Based on our thorough stochastic simulation. We believe that these results provide fresh insights into the midinfrared amplitude-squeezed light source and also intriguing applications in numberless areas such as free-space CV QKD communication. Further work will focus on several aspects. The first one is to improve our ICL model by the equivalent circuit approach since we consider only one carrier reservoir and the ICLs' electrical characteristics are not exactly entailed. The second one is the experimental investigation of squeezed light with midinfrared quantum cascade photonic devices in order to verify our predictions and we will endeavor to realize the designed free-space CV QKD system. Last but not least, we believe that ICL frequency combs can be also considered useful to engineer squeezed and color entangled states in the midinfrared domain [53].

ACKNOWLEDGMENTS

The authors wish to thank Professor Jesper Mørk from Technical University of Denmark for useful discussions.

[1] H. Haken, *Laser Light Dynamics* (North-Holland Publishing Co., Amsterdam, 1985), Vol. 2.
[2] W. H. Louisell, *Quantum Statistical Properties of Radiation* (John Wiley and Sons, Inc., New York, 1973).
[3] M. O. Scully and W. E. Lamb, Quantum theory of an optical maser. I. General theory, Phys. Rev. **159**, 208 (1967).
[4] R. J. Glauber, Coherent and incoherent states of the radiation field, Phys. Rev. **131**, 2766 (1963).
[5] S. Machida and Y. Yamamoto, Quantum-limited operation of balanced mixer homodyne and heterodyne receivers, IEEE J. Quantum Electron. **22**, 617 (1986).
[6] H. P. Yuen and V. W. S. Chan, Noise in homodyne and heterodyne detection, Opt. Lett. **8**, 177 (1983).
[7] H. P. Yuen, Two-photon coherent states of the radiation field, Phys. Rev. A **13**, 2226 (1976).
[8] D. F. Walls, Squeezed states of light, Nature **306**, 141 (1983).
[9] C. Weedbrook, S. Pirandola, R. García-Patrón, N. J. Cerf, T. C. Ralph, J. H. Shapiro, and S. Lloyd, Gaussian quantum information, Rev. Mod. Phys. **84**, 621 (2012).
[10] B. J. Lawrie, P. D. Lett, A. M. Marino, and R. C. Pooser, Quantum sensing with squeezed light, ACS Photonics **6**, 1307 (2019).
[11] H. Yuen and J. Shapiro, Optical communication with two-photon coherent states–Part I: Quantum-state propagation and quantum-noise, IEEE Trans. Inf. Theory **24**, 657 (1978).
[12] R. E. Slusher, L. W. Hollberg, B. Yurke, J. C. Mertz, and J. F. Valley, Observation of Squeezed States Generated by Four-Wave Mixing in an Optical Cavity, Phys. Rev. Lett. **55**, 2409 (1985).

[13] L.-A. Wu, H. J. Kimble, J. L. Hall, and H. Wu, Generation of Squeezed States by Parametric Down Conversion, Phys. Rev. Lett. **57**, 2520 (1986).

[14] Y. Yamamoto, S. Machida, and O. Nilsson, Amplitude squeezing in a pump-noise-suppressed laser oscillator, Phys. Rev. A **34**, 4025 (1986).

[15] S. Machida, Y. Yamamoto, and Y. Itaya, Observation of Amplitude Squeezing in a Constant-Current-Driven Semiconductor Laser, Phys. Rev. Lett. **58**, 1000 (1987).

[16] H. Wang, M. J. Freeman, and D. G. Steel, Squeezed Light from Injection-Locked Quantum Well Lasers, Phys. Rev. Lett. **71**, 3951 (1993).

[17] D. C. Kilper, P. A. Roos, J. L. Carlsten, and K. L. Lear, Squeezed light generated by a microcavity laser, Phys. Rev. A **55**, R3323 (1997).

[18] T. Gensty, W. Elsäßer, and C. Mann, Intensity noise properties of quantum cascade lasers, Opt. Express **13**, 2032 (2005).

[19] R. Q. Yang, Infrared laser based on intersubband transitions in quantum wells, Superlattices Microstruct. **17**, 77 (1995).

[20] A. Delga and L. Leviandier, in *Quantum Sensing and Nano Electronics and Photonics XVI*, Vol. 10926 (SPIE, 2019).

[21] O. Spitz, P. Didier, L. Durupt, D. A. Díaz-Thomas, A. N. Baranov, L. Cerutti, and F. Grillot, Free-space communication with directly modulated mid-infrared quantum cascade devices, IEEE J. Sel. Top. Quantum Electron. **28**, 1 (2022).

[22] V. Scarani, H. Bechmann-Pasquinucci, N. J. Cerf, M. Dušek, N. Lütkenhaus, and M. Peev, The security of practical quantum key distribution, Rev. Mod. Phys. **81**, 1301 (2009).

[23] C. S. Jacobsen, L. S. Madsen, V. C. Usenko, R. Filip, and U. L. Andersen, Complete elimination of information leakage in continuous-variable quantum communication channels, Npj Quantum Inf. **4**, 1 (2018).

[24] N. Hosseinidehaj, M. S. Winnel, and T. C. Ralph, Simple and loss-tolerant free-space quantum key distribution using a squeezed laser, Phys. Rev. A **105**, 032602 (2022).

[25] D. Vasylyev, A. A. Semenov, W. Vogel, K. Günthner, A. Thurn, Ö. Bayraktar, and C. Marquardt, Free-space quantum links under diverse weather conditions, Phys. Rev. A **96**, 043856 (2017).

[26] F. Grosshans, G. Van Assche, J. Wenger, R. Brouri, N. J. Cerf, and P. Grangier, Quantum key distribution using Gaussian-modulated coherent states, Nature **421**, 238 (2003).

[27] S. Zhao and F. Grillot, Modeling of amplitude squeezing in a pump-noise-suppressed interband cascade laser, IEEE Photonics J. **14**, 1 (2022).

[28] J.-L. Vey and P. Gallion, Semiclassical model of semiconductor laser noise and amplitude noise squeezing. I. Description and application to Fabry-Perot laser, IEEE J. Quantum Electron. **33**, 2097 (1997).

[29] J. Mørk and G. L. Lippi, Rate equation description of quantum noise in nanolasers with few emitters, Appl. Phys. Lett. **112**, 141103 (2018).

[30] J. Mørk and K. Yvind, Squeezing of intensity noise in nanolasers and nanoLEDs with extreme dielectric confinement, Optica **7**, 1641 (2020).

[31] A. Vallet, L. Chusseau, F. Philippe, and A. Jean-Marie, Markov model of quantum fluctuations at the transition to lasing of semiconductor nanolasers, Physica E: Low-Dimensional Syst. Nanostruct. **105**, 97 (2019).

[32] L. A. Coldren, S. W. Corzine, and M. L. Mashanovitch, *Diode Lasers and Photonic Integrated Circuits* (John Wiley & Sons, Inc., Hoboken, New Jersey, 2012).

[33] A. Lebreton, I. Abram, N. Takemura, M. Kuwata-Gonokami, I. Robert-Philip, and A. Beveratos, Stochastically sustained population oscillations in high-β nanolasers, New J. Phys. **15**, 033039 (2013).

[34] G. P. Puccioni and G. L. Lippi, Stochastic simulator for modeling the transition to lasing, Opt. Express **23**, 2369 (2015).

[35] K. Roy-Choudhury, S. Haas, and A. F. J. Levi, Quantum Fluctuations in Small Lasers, Phys. Rev. Lett. **102**, 053902 (2009).

[36] K. Roy-Choudhury and A. F. J. Levi, Quantum fluctuations in very small laser diodes, Phys. Rev. A **81**, 013827 (2010).

[37] Y. Deng and C. Wang, Rate equation modeling of interband cascade lasers on modulation and noise dynamics, IEEE J. Quantum Electron. **56**, 1 (2020).

[38] E. C. André, J. Mørk, and M. Wubs, Efficient stochastic simulation of rate equations and photon statistics of nanolasers, Opt. Express **28**, 32632 (2020).

[39] C. Gies, J. Wiersig, M. Lorke, and F. Jahnke, Semiconductor model for quantum-dot-based microcavity lasers, Phys. Rev. A **75**, 013803 (2007).

[40] W. W. Chow and S. Reitzenstein, Quantum-optical influences in optoelectronics–an introduction, Applied Physics Reviews **5**, 041302 (2018).

[41] Y. Lien, S. M. de Vries, N. J. van Druten, M. P. van Exter, and J. P. Woerdman, Photon Statistics of a Laser with Slow Inversion, Phys. Rev. Lett. **86**, 2786 (2001).

[42] U. L. Andersen, T. Gehring, C. Marquardt, and G. Leuchs, 30 years of squeezed light generation, Physica Scripta **91**, 053001 (2016).

[43] T. Kashiwazaki, N. Takanashi, T. Yamashima, T. Kazama, K. Enbutsu, R. Kasahara, T. Umeki, and A. Furusawa, Continuous-wave 6-dB-squeezed light with 2.5-THz-bandwidth from single-mode PPLN waveguide, APL Photonics **5**, 036104 (2020).

[44] Y. Zhao, Y. Okawachi, J. K. Jang, X. Ji, M. Lipson, and A. L. Gaeta, Near-Degenerate Quadrature-Squeezed Vacuum Generation on a Silicon-Nitride Chip, Phys. Rev. Lett. **124**, 193601 (2020).

[45] A. H. Safavi-Naeini, S. Gröblacher, J. T. Hill, J. Chan, M. Aspelmeyer, and O. Painter, Squeezed light from a silicon micromechanical resonator, Nature **500**, 185 (2013).

[46] P. Didier, O. Spitz, L. Cerutti, D. A. Diaz-Thomas, A. N. Baranov, M. Carras, and F. Grillot, Relative intensity noise and intrinsic properties of rf mounted interband cascade laser, Appl. Phys. Lett. **119**, 171107 (2021).

[47] Y. Lin, L. Li, W. Huang, R. Q. Yang, J. A. Gupta, and W. Zheng, Quasi-Fermi level pinning in interband cascade lasers, IEEE J. Quantum Electron. **56**, 1 (2020).

[48] J. R. Meyer, W. W. Bewley, C. L. Canedy, C. S. Kim, M. Kim, C. D. Merritt, and I. Vurgaftman, The interband cascade laser, Photonics **7**, 75 (2020).

[49] S. Machida and Y. Yamamoto, Ultrabroadband Amplitude Squeezing in a Semiconductor Laser, Phys. Rev. Lett. **60**, 792 (1988).

[50] R. Short and L. Mandel, Observation of Sub-Poissonian Photon Statistics, Phys. Rev. Lett. **51**, 384 (1983).

[51] M. A. Carroll, G. D'Alessandro, G. L. Lippi, G.-L. Oppo, and F. Papoff, Photon-number squeezing in nano- and microlasers, Appl. Phys. Lett. **119**, 101102 (2021).

[52] M. A. Carroll, G. D'Alessandro, G. L. Lippi, G.-L. Oppo, and F. Papoff, Thermal, Quantum Antibunching and Lasing Thresholds from Single Emitters to Macroscopic Devices, Phys. Rev. Lett. **126**, 063902 (2021).

[53] L. A. Sterczewski, M. Bagheri, C. Frez, C. L. Canedy, I. Vurgaftman, M. Kim, C. S. Kim, C. D. Merritt, W. W. Bewley, and J. R. Meyer, Interband cascade laser frequency combs, Journal of Physics: Photonics **3**, 042003 (2021).